Proceedings of the 9th International Conference of Control Systems, and Robotics (CDSR'22)
Niagara Falls, Canada – June 02-04, 2022
Paper No. 109
DOI: 10.11159/cdsr22.109

Magnetic Drive-Trains Pole-Slipping Inducements and Overload Speed Reduction

Xiaowen Liao[1], Chris Bingham[2], Tim Smith[2]
[1] Guangdong University of Petrochemical Technology (GDUPT), and Joint Research Lab between GDUPT and University of Lincoln
Guandu 2 road, Maoming, China
Xliao@lincoln.ac.uk
[2]School of Engineering, University of Lincoln
Brayford pool, Lincoln, UK
Cbingham@lincoln.ac.uk, Tismith@lincoln.ac.uk

Abstract - The paper presents an analysis of magnetic drive train (MDT) pole-slipping and an amelioration strategy to reduce uncontrolled load-side speed when subject to pole-slipping. Initially, the pole-slipping inducements of MDTs are deduced based on the assumption that driving controllers are designed with sufficient servo rigidity. Subsequently, in order to avoid initiating degrading coupling torque oscillations, the transient response of the induced coupling torque is analysed. Next, the paper provides a load-side speed reduction methodology based on load-side speed estimation, synchronization, and piecewise electromagnetic torque excitation to reduce the potential for (mechanical or temperature induced) damage to mechanical components (eg. bearings) as a result of uncontrolled speed during pole-slipping. More generally, consideration of electromagnetic torque production for flexible systems, such as MDTs, possessing variable/nonlinear stiffness, is addressed to ameliorate the chances of inducing pole-slipping.

***Keywords*:** Magnetic drive-trains, pole-slipping, inducements, speed reduction, overload conditions

1. Introduction

Drive-trains integrating magnetic torque transfer components, such as magnetic gears or magnetic couplings, offer physical isolation between primary driving and driven shafts, thereby eliminating some of the disadvantages commonly to attributed to traditional mechanical power transmission systems, such as overload failures, jamming, mechanic fatigue and regular maintenance requirements [1][2].

However, the magnetic drive-train (MDT) has the potential for torque transmission 'slip' (termed pole-slipping), in which the driving shaft loses synchronization with the driven-side. Due to cost, integration and isolation issues, measurements of load-side speed and position can be prohibitive in practice, meaning that pole-slipping can be challenging to detect. It is therefore crucial for designers to understand the modes of inducing pole-slipping when designing (typically speed) controllers. [2][3][4] attribute pole-slipping to overload torque whilst [5] observes that an abrupt change in speed references or load-torque initiates pole-slipping. However, these studies lack a more formal mathematical analysis of pole-slipping inducement mode.

Control methods proposed by [3][4] require non-reversible mechanical devices, such as worm gear or lead screw drives to be incorporated in MDTs, thereby preventing the driven shaft from operating at an anomalously high speed. As a result, controllers cannot immediately sense load conditions when the overload (torque) condition is removed due to the lack of load side measurements.

By contrast, [2][5] [6][7] employ direct drive modes, which provide a fast response with simple design and can indirectly sense the variation of load-side torque through output control effort. Nevertheless, an impediment to applying MDTs in direct drive applications is that the load-side speed can become uncontrolled during overload conditions. Mechanical elements such as bearings employed in drive-trains have permissible maximum operating temperatures, and if excessive load-side speed cannot be sufficiently controlled, the resulting high temperatures will induce abnormal wear and damage. Speed reduction control when pole-slipping has yet to be addressed in previous studies. Here then, it is shown that if the primary-side drive can effectively develop electromagnetic torque as a damping mechanism to the overload

component, the load-side speed can then be reduced. However, applying electromagnetic excitations can create substantial coupling torque oscillations, resulting in further de-synchronization. Command generation methods [8][9][10] use a-prior knowledge of flexible systems to provide piecewise excitation reference demand solutions; consequently, the oscillatory amplitude of torsional torque can be greatly reduced. However, unlike common resilient-systems, the torsional stiffness of MDTs varies with electromagnetic and load torque excitation.

This paper therefore provides an analysis of pole-slipping inducement and reduces load-side (uncontrolled) shaft speed during overload (pole-slipping) conditions for direct drive MDTs. Overload torque is the most commonly accepted cause of pole-slipping and is addressed elsewhere in literature; hence it is not specifically considered in isolation here. Assuming the driving controller is designed with sufficient servo rigidity, load-side dynamics are used to identify and analyse the inducement of pole-slipping. Motivated by [8][9], this paper examines the transient response of coupling torque of a running MDT under electromagnetic excitations. The characteristics of the transient responses are then applied to reduce torsional torque oscillations—through applying piecewise electromagnetic inputs. Finally, a speed reduction methodology based on a command generation method and a case study, are presented.

2. Dynamics of Magnetic Drive-Trains

To provide a practical focus for the investigation, the magnetic drive-train studied in the paper has 5 pole pairs (p) and a maximum (pull-out) torque (T_G) of 1.6 N·m; the load- and motor-side inertias (J_L and J_M) are 0.001 kg·m^2, and the load- and motor-side friction coefficient (B_L and B_M) are 0.003 N·m/(rad/s). θ_M and θ_L are denoted as the positions of motor- and load-side shafts. K_{lin} is denoted as the torsional stiffness linearized at operating points, and K_{lin} is given by [2]:

$$K_{\text{lin}} = T_G p \cos(p\theta_D) \tag{1}$$

where $\theta_D = \theta_M - \theta_L$ is the relative mechanical displacement angle. Consequently, we can analyse MDTs from the perspective of classical two-mass systems. The anti-resonant frequency (ω_a) and resonant frequency (ω_n) are described by:

$$\omega_a = \sqrt{\frac{K_{\text{lin}}}{J_L}}, \qquad \omega_n = \sqrt{\frac{K_{\text{lin}}(1+R)}{J_L}} \tag{2}$$

where R is the inertia ratio ($R = J_L/J_M$), and the coupling torque (T_C) is given by:

$$T_C = K_{\text{lin}}\theta_D \tag{3}$$

If damping torque is neglected, the MDT dynamics are described by

$$\begin{aligned} \dot{\theta}_M &= \omega_M \\ \dot{\omega}_M &= (T_{em} - T_C - B_M\omega_M)/J_M \\ \dot{\theta}_L &= \omega_L \\ \dot{\omega}_L &= (T_C - T_L - B_L\omega_L)/J_L \end{aligned} \tag{4}$$

where T_{em} and T_L are the electromagnetic torque and load torque; ω_M and ω_L are the speed of the motor- and load-side components; B_M and B_L are the friction coefficients of the motor- and load-side shafts.

3. Inducement of Pole-Slipping

Substituting (3) into (4), yields

$$\dot{\omega}_L = (K_{\text{lin}}\theta_D - B_L\omega_L - T_L)/J_L \tag{5}$$

In this case a model of the (load-side) dynamic system can be described as in Fig.1.

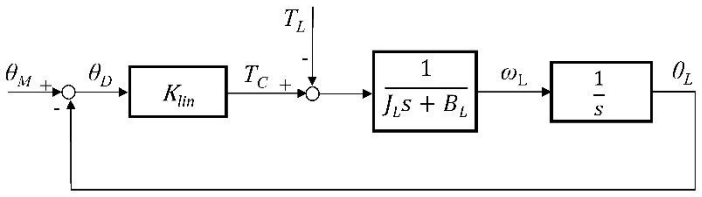

Fig.1: Load-side dynamics

Now, assuming θ_M and T_L are inputs, and θ_L is an output, the load-side dynamics can be written as:

$$\begin{bmatrix}\dot{\omega}_L \\ \dot{\theta}_L\end{bmatrix} = \begin{bmatrix}-B_L/J_L & -K_{lin}/J_L \\ 1 & 0\end{bmatrix}\begin{bmatrix}\omega_L \\ \theta_L\end{bmatrix} + \begin{bmatrix}K_{lin}/J_L & -1/J_L \\ 0 & 0\end{bmatrix}\begin{bmatrix}\theta_M \\ T_L\end{bmatrix} \tag{6}$$

$$\theta_L = [0 \quad 1]\begin{bmatrix}\omega_L \\ \theta_L\end{bmatrix} \tag{7}$$

The criterion for preventing MDT pole-slipping is $|\theta_M - \theta_L| < \pi/2p$; therefore, the impact of the input position θ_M and the load-torque T_L should be carefully considered. According to (6) and (7), the relation between T_L, θ_M and θ_L can be described as:

$$\theta_L(s) = \frac{K_{\text{lin}}}{J_L s^2 + B_L s + K_{\text{lin}}}\theta_M(s) - \frac{1}{J_L s^2 + B_L s + K_{\text{lin}}}T_L(s) \tag{8}$$

Letting $\theta_D(s)$ denote $\theta_M(s) - \theta_L(s)$, $\theta_D(s)$ can then be obtained from (8) as follows:

$$\theta_D(s) = \frac{(J_L s^2 + B_L s)\theta_M(s) + T_L(s)}{J_L s^2 + B_L s + K_{\text{lin}}} \tag{9}$$

It is well known from previous studies [2][3][4] that MDTs enter a pole-slipping regime when an aggressive load torque (T_L) occurs. Here, supposing the variation of T_L is small, and the driving-side controller is designed with sufficient servo rigidity, the motor-side position (θ_M) is therefore only governed by the reference speed ω_{ref} and the design of a low-pass pre-filter placed between the speed references and speed controllers (Fig. 2 shows the control scheme that is commonly used, where $1/(1+\tau_1 s)$ and $F_c(s)$ denote the low-pass filter and speed controller, respectively), and $\theta_M(s)$ is given by:

$$\theta_M(s) = \frac{\omega_{ref}(s)}{s(1+\tau_1 s)} \tag{10}$$

where τ_1 is the time constant of the low-pass filter. Substituting (10) into (9), gives

$$\theta_D(s) = \frac{J_L \omega_{ref}(s) s^2 + \big(\tau_1 T_L(s) s + T_L(s)\big)s + B_L \omega_{ref}(s)}{(s+\tau_1 s^2)(J_L s^2 + B_L s + K_{\text{lin}})} \tag{11}$$

Supposing $\tau_1 = 0.1$ s and the controller bandwidth $\omega_c = 10$ rad/s (for the MDT under 99% of the pull-out torque, $\omega_a = 33.6$ rad/s, $\omega_n = 48.4$ rad/s), (11) simplifies to

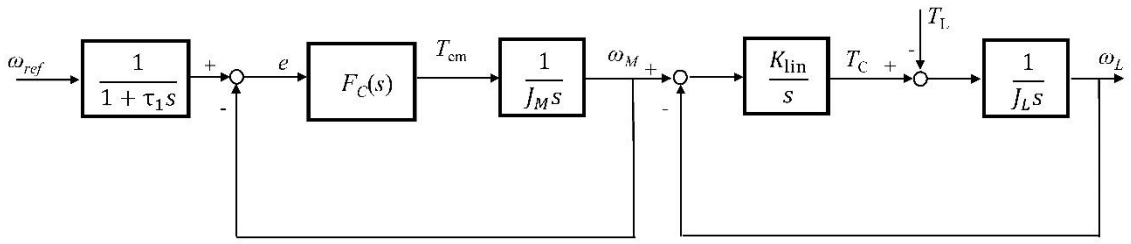

Fig. 2: Control scheme

$$\theta_D(s) = \frac{J_L \omega_{ref}(s) s^2 + \left(\tau_1 T_L(s) s + T_L(s)\right) s}{(\tau_1 s^2 + s) K_{\text{lin}}} \tag{12}$$

Modelling $\omega_{ref}(s)$ and $T_L(s)$ as step inputs represented by $\omega_{ref}(s) = \omega_{ref}/s$ and $T_L(s) = T_L/s$, respectively, (12) then reduces to

$$\theta_D(s) = \frac{J_L \omega_{ref}}{(\tau_1 s + 1) K_{\text{lin}}} + \frac{T_L}{s K_{\text{lin}}} \tag{13}$$

Inversing Laplace transforming (13), yields

$$\theta_D(t) = \frac{J_L \omega_{ref}}{\tau_1 K_{\text{lin}}} e^{-\frac{1}{\tau_1} t} + \frac{T_L}{K_{\text{lin}}} \tag{14}$$

Equation (14) shows that if friction coefficients are not taken into consideration, the relative displacement angle resulting from T_L and ω_{ref} takes form of a constant and an exponential damping term, respectively. Although using the low-pass filter can suppress speed oscillations resulting from speed references, (14) indicates that an improper speed command or an overly-small time constant choice will lead the MDT to pole-slip. In particular, a small increment of ω_{ref} will result in a pole-slipping anomaly when MDTs are operating under high load torque conditions (K_{lin} decreases as load torque increases).

4. Reduce Coupling Torque Oscillations via Appropriate Command Generation

To accommodate appropriate speed control when pole-slipping, it is important that coupling torque oscillations are reduced. Without this, θ_D may transiently exceed its normal operating bounds and further induce pole-slipping. For most applications of MDTs, the coupling torque will not be measured directly. To show the characteristics of transient coupling terms response, a simulation model has been constructed based on the parameters specified in Section 2 (the input electromagnetic torque (T_{em}) and load torque (T_L) are set to 1 N·m and 0 N·m, respectively).

Fig. 3 shows that the coupling torque in response to T_{em} takes the form of an exponentially decaying oscillation, described by

$$x(t) = x_0 e^{-\sigma t} \cos(\omega_n t + \varphi) \tag{15}$$

where σ is the decay rate, ω_n is the resonant frequency, φ is the phase angle, x_0 and $x(t)$ represent the initial amplitude and the amplitude at time t, respectively. Letting T_{cs} denote the steady-state value of coupling torque, according to (1), (2), the damped period of the MDT dynamics is given by

$$T_d = \frac{2\pi}{\omega_n} = 2\pi \sqrt{\frac{J_L}{T_G p (1+R) \cos(\arcsin(T_{cs}/T_G))}} \tag{16}$$

It can be seen from Fig. 2 that $T_d = 0.05$ s, which aligns with (16). Moreover, Fig. 3 shows that the MDT needs $0.5T_d$ to reach its first positive peak and a further $0.5T_d$ to approach the first negative peak (assuming the DC offset is subtracted from the damped sinusoid), and that the decay rate σ is relatively low. This means that if a T_{em} is imposed in a

piecewise manner at time t and $t + 0.5T_d$, respectively, the oscillation of coupling torque caused by the first step excitation can be greatly reduced by the second application. This principle is verified by the simulation results shown in Fig. 4.

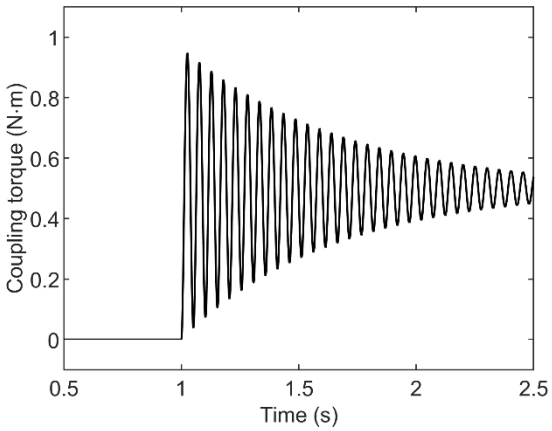

Fig. 3: Transient response of T_C under step references ($T_{em} = 1$ N·m, $T_L = 0$ N·m).

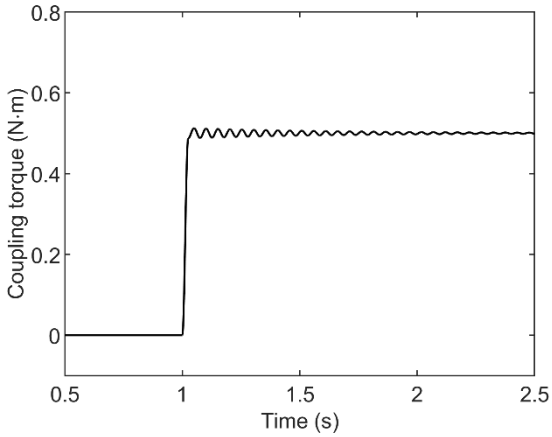

Fig. 4: Transient response of T_C under step references ($T_L = 0$ N · m; $T_{em} = 0.5$ N · m, 1 N · m at 1-1.025 s and 1.025-2.5 s, respectively)

5. Speed Reduction during Overload Anomalies

The proposed speed reduction strategy considered here is based on the command generation principle discussed in the previous section, and the strategy includes load-side speed estimation, synchronization, and appropriate electromagnetic torque excitation.

Initially, it is proposed to estimate load-side running speed through primary motor-side speed oscillations or control output variations. The frequency of oscillation reflects the relative rotating speed of magnetic field generated by driving and driven magnetically coupled sides of the drive-train. Here then, supposing the frequency of modulation is ω_f (Hz), the speed of motor-side is ω_{M_rmin}(the unit is rpm), the load-side speed can then be estimated from

$$\omega_{L\_rmin} = -\omega_{M\_rmin} - \omega_f * 60/p \tag{17}$$

It is now proposed to control the shaft of primary driven (motor) side to synchronize with the load-side speed which is free-running during overload conditions. When both sides are synchronized, the excitation torque T_{em} can then be used to estimate the value of overload torque, described by

$$T_L = -T_{em} - B_M \omega_M + B_L \omega_M \tag{18}$$

Finally, we now employ the command generation method (seen previously) to piecewise impose the required excitation torque, resulting in load-side speed reduction. Letting T_{emf} represents the final value of T_{em} after a speed reduction, then (19) holds.

$$T_L - T_C = T_C - T_{emf} \tag{19}$$

and T_c at this moment should reach or be a slightly lower than the maximum coupling torque (T_G). Hence, T_{emf} is given by

$$T_{emf} = 2T_C - T_L \tag{20}$$

The excitation should piecewise increase to T_{emf}. However, the torsional stiffness of MDTs varies with electromagnetic and load-torque excitations, resulting in variable damped periods of oscillation. Letting T_{csi} denotes the steady-state value of coupling torque after the i th excitation, then, T_{csi} is described by

$$T_{csi} = (T_{emi} + T_L)/2 \tag{21}$$

where T_{emi} represents the summarized increment of T_{em} after the i th excitation. Then, (16) can be used to calculate the i th damp period with (21).

An example of how to use the principles set out above to achieve an overload protection strategy, is now given. For the MDT prototype studied in the paper, $\omega_a = 44.1$ rad/s, $\omega_n = 62.8$ rad/s under 97% of pull-out torque. Let the time constant of the pre-filter be equal to the damped period of the MDT, i.e., $1/(0.1s + 1)$, and the speed controller is designed as a common PI regulator with $K_p = 3.97, K_i = 3.17$ (giving a resulting bandwidth of 5 rad/s). Fig. 5 shows the results of a scenario of the simulated system, regulated by the classical PI speed controller operating normally between 0-10s and is then subject to an overload torque ($T_L = 2T_G$) after 10 s.

(1) Load-side speed estimation

It can be seen from Fig. 5 and Fig. 6 that the motor-side shaft maintains its speed when pole-slipping occurs and that both-sides of the MDT oscillate at same frequency. Fig. 7 provides a Fast Fourier Transform (FFT) of the motor-side shaft speed which shows that the dominant frequency is 915.5 Hz and that the amplitude of speed oscillations is approximately 2 rpm. According to (17), the calculated load-side speed is then −11786 rpm, which aligns with the result in Fig. 5.

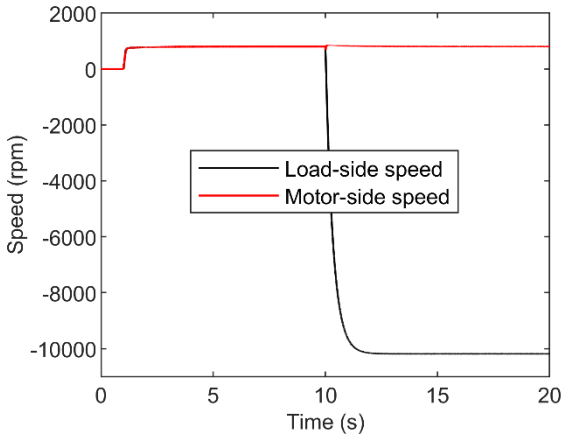

Fig. 5: Simulated speed before and during the overload condition (the motor-side reference speed r =800 rpm at 1-20s, T_L= 0 N·m at 0-10s, T_L = $2T_G$ at 10-20s, respectively).

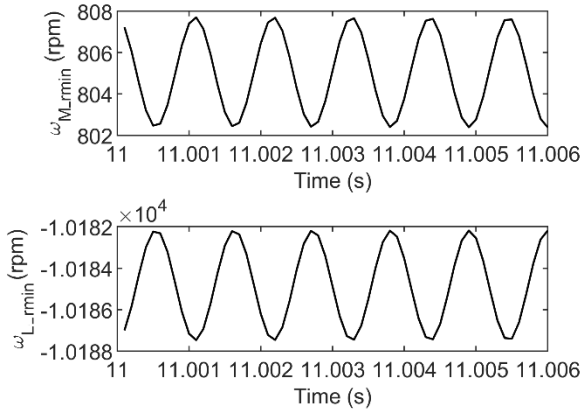

Fig. 6: Simulated speed of the both-side couplings during over-load slipping.

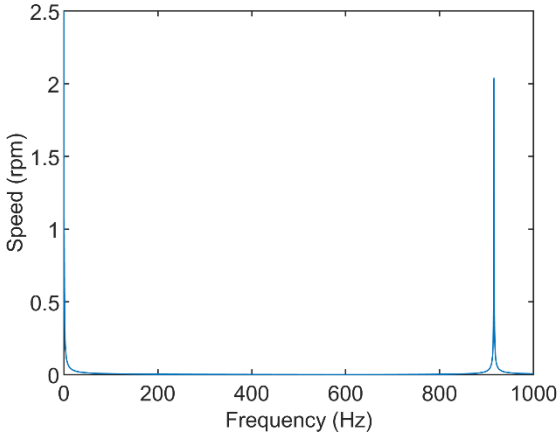

Fig. 7: Single-sided amplitude spectrum of motor-side speed

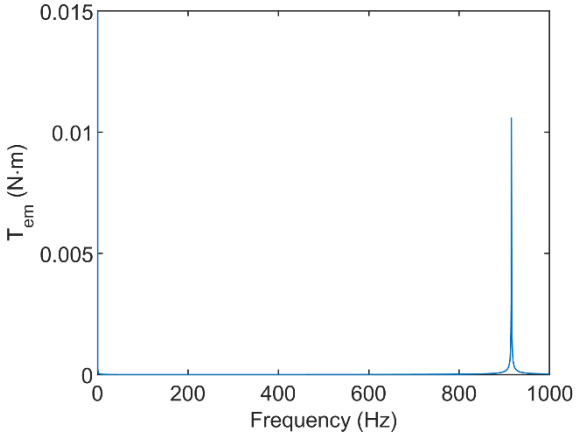

Fig. 8: Single-sided amplitude spectrum of T_{em}

Fig. 8 also shows the FFT of T_{em} during pole-slipping, and shows that ω_f could also be obtained from small variations in control effort (albeit this will be dependent of controller and system bandwidth in general).

(2) Synchronization and speed reduction

With the identified load-side speed now used as the driven speed reference, the motor-side shaft can now be regulated to synchronize with the load-side speed. The motor-side control effort T_{em} effectively now behaves as a 'load-torque'. The steady value of T_{em} under synchronization is $-2T_G$ (see Fig. 9). Hence, $T_L = 2T_G (see\ (18))$ Taking the oscillations of coupling torque into consideration, suppose $T_C = T_G - 0.1$ N·m after the speed reduction (in this case). Then, according to (20), the final value of T_{emf} after the speed reduction is -0.2 N·m. This means that the excitation is required to be raised from -3.2 N·m ($2T_G$) to -0.2 N·m. Hence, according to the rule of command generation, this 3 N·m increment is piecewise described by:

$$T_{em} = \frac{1}{s}\left(0.75 + 1.5e^{-\frac{1}{2}T_{d1}s} + 0.75e^{-\frac{1}{2}T_{d2}s}\right) - 3.2 \tag{22}$$

where T_{d1} and T_{d2} are the damped periods calculated by (16). According to (16) and (21), $T_{d1} = 0.04$ s, $T_{d2} = 0.09$ s.

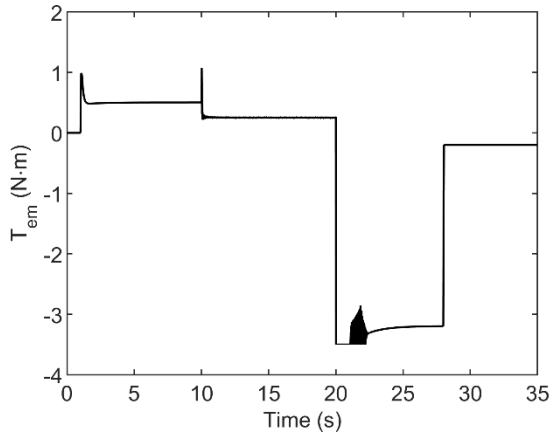

Fig. 9: Simulation results of control effort before and during the overload condition.

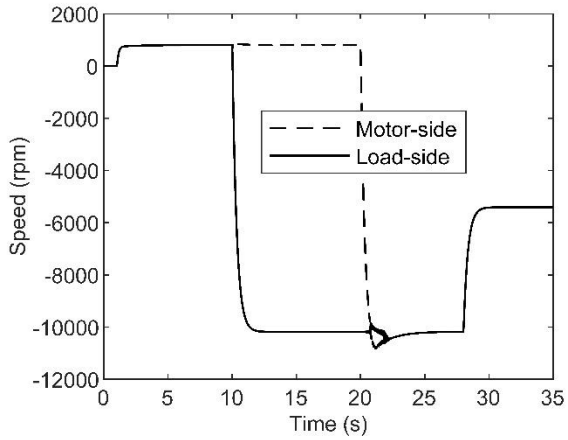

Fig. 10: Simulation results of running speed before and during the overload condition (the MDT is normal running at 1-10s, T_L= 0 at 0-10s, $T_L = 2T_G$ at 10-35s, respectively).

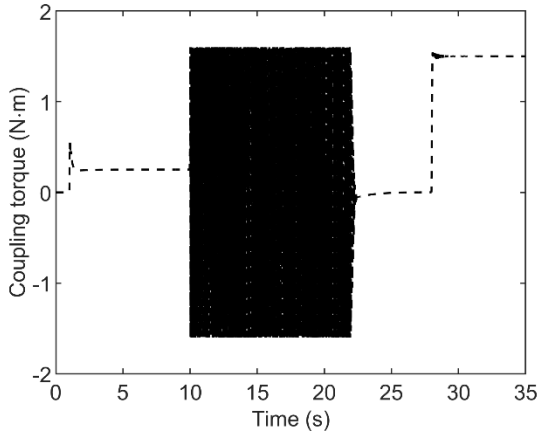

Fig. 11: Simulation results of coupling torque before and during the overload condition.

Fig. 10 shows the simulation results of a whole running process of the MDT system, including normal operation, pole-slipping, synchronization and speed reduction. It can be seen from Fig. 9 and Fig. 11 that speed reduction begins at 28 s and the load-side speed decreases from ~10,000 rpm to ~5,000 rpm. As shown in Fig. 11, the coupling torque oscillations

have been suppressed with the choice of piecewise T_{em} inputs; consequently, the speed of both-sides of the MDT avoid significant oscillations (see Fig. 10).

4. Conclusion

Through discussions of pole-slipping, the transient response of coupling torque and a speed reduction methodology based on piecewise reference command generation, a key issue for the deployment of MDTs for direct drive applications has been addressed. The analysis of the load-side dynamics shows that the variations of displacement angle between driving and driven shafts are associated with load-torque disturbances, speed references and the time constant choice of reference pre-filters. In particular, it is shown that uninhibited reference commands can immediately send MDTs into pole-slipping with common PI speed control configurations. Moreover, coupling torque transient responses of MDTs under step excitations indicate that the speed/coupling torque oscillations can be reduced by piecewise applying electromagnetic torque excitations, and the proposed speed reduction methodology can ameliorate the detrimental effects of uncontrolled load-side speed when in the pole-slipping regime.

References

[1] Y. Wang, M. Filippini, N. Bianchi and P. Alotto, "A Review on Magnetic Gears: Topologies, Computational Models, and Design Aspects," in *IEEE Transactions on Industry Applications*, vol. 55, no. 5, pp. 4557-4566, 2019.

[2] R. Montague, C. Bingham and K. Atallah, "Servo Control of Magnetic Gears," in *IEEE/ASME Transactions on Mechatronics*, vol. 17, no. 2, pp. 269-278, 2012.

[3] M. Bouheraoua, J. Wang and K. Atallah, "Slip Recovery and Prevention in Pseudo Direct Drive Permanent-Magnet Machines," in *IEEE Transactions on Industry Applications*, vol. 51, no. 3, pp. 2291-2299, 2015.

[4] M. Bouheraoua, J. Wang and K. Atallah, "Design and implementation of an observer-based state feedback controller for a pseudo direct drive." *IET Electric Power Applications*, vol. 7, no. 7, pp. 643-653, 2013.

[5] R. Montague, C. Bingham and K. Atallah, "Magnetic Gear Pole-Slip Prevention Using Explicit Model Predictive Control," in *IEEE/ASME Transactions on Mechatronics*, vol. 18, no. 5, pp. 1535-1543, 2013.

[6] Montague, Ryan, and Chris Bingham, "Nonlinear control of magnetically-geared drive-trains," *International Journal of Automation and Computing*, vol. 10, no. 4, pp. 319-326, 2013.

[7] X. Liao, C. Bingham, A. Zolotas, Q. Zhang and T. Smith, "Speed control of drive-train incorporating magnetic coupling," International *Conference on Electrical Machines*, Gothenburg, Sweden, 2020, pp. 1225-1231.

[8] S. William, "Command shaping for flexible systems: A review of the first 50 years," *International journal of precision engineering and manufacturing*, vol. 10, no. 4, pp.153-168, 2009.

[9] S. William, R. Eloundou, and J. Lawrence, "Command generation for flexible systems by input shaping and command smoothing," *Journal of guidance, control, and dynamics*, vol.33, no. 6, pp. 1697-1707, 2010.

[10] M. O.T. Cole, P. Shinonawanik, and T. Wongratanaphisan, "Time-domain prefilter design for enhanced tracking and vibration suppression in machine motion control." *Mechanical Systems and Signal Processing*, vol. 10, no.4, pp. 106-119, 2018.